DOI: 10.24850/j-tyca-13-06-06

Articles

Shoreline analysis and erosion risk assessment of a coastal strip subjected to high anthropogenic pressure

Análisis de la línea de costa y evaluación del riesgo de erosión de una franja costera sometida a alta presión antrópica

Yedid Zambrano-Medina[1], ORCID: https://orcid.org/0000-0001-8820-0688

Cuauhtémoc Franco-Ochoa[2], ORCID: https://orcid.org/0000-0002-7554-3603

Wenseslao Plata-Rocha[3], ORCID: https://orcid.org/0000-0002-9469-7886

Fernando García-Páez[4]

Miguel Montoya-Rodríguez[5]

Edgar Mendoza-Baldwin[6], ORCID: https://orcid.org/0000-0002-1991-4721

[1]Facultad de Ciencias de la Tierra y el Espacio, Universidad Autónoma de Sinaloa, Culiacán, Sinaloa, México, yedidzambrano@uas.edu.mx

[2]Facultad de Ingeniería Civil, Universidad Autónoma de Sinaloa, Culiacán, Sinaloa, México, cfrancoo@uas.edu.mx

[3]Facultad de Ciencias de la Tierra y el Espacio, Universidad Autónoma de Sinaloa, Culiacán, Sinaloa, México, wenses@uas.edu.mx

[4]Facultad de Ingeniería Civil, Universidad Autónoma de Sinaloa, Culiacán, Sinaloa, México, garpaez@uas.uasnet.mx

[5]Departamento de Ingeniería Portuaria y Sistemas Geoespaciales, Instituto Mexicano del Transporte, Querétaro, México, mmontoya@imt.mx

[6]Instituto de Ingeniería, Universidad Nacional Autónoma de México, México, emendozab@ii.unam.mx

Corresponding author: Cuauhtémoc Franco-Ochoa, cfrancoo@uas.edu.mx

Abstract

This study aims to understand the role of key drivers of historical changes in the shoreline and its implications with the erosion risk in the northern coastal strip of the state of Sinaloa, located on the east coast of the Gulf

of California. Digital maps from different years (1981, 1991, 2004, and 2018) are analyzed using geographic information system software (DSAS and CERA) to examine: (a) the movement and rate of the shoreline change; and (b) the potential vulnerability consequences, and erosion risk. The obtained results indicate that between 1981 and 2018: (a) anthropogenic actions (dams and breakwaters) were the main drivers of both the shoreline changes and the environmental damage underlying the erosion risk that has occurred in recent decades; (b) the coastline of the study area has been eroding with an average EPR of -3.1 m per year, which has led to an average NSM of -112.9 m; and (c) the risk of erosion remained moderate, although the vulnerability increased from a moderate to a high level and potential consequences from a very low to a moderate level. Besides, the results of this study provide a basis for future analyses focused on predicting shoreline changes and coastal risk.

Keywords: coastal erosion, DSAS, CERA, coastal risk, vulnerability, Gulf of California.

Resumen

El objetivo de este estudio es entender el papel de los principales impulsores de los cambios históricos de la línea de costa y sus implicaciones en el riesgo de erosión en una franja costera al norte del estado de Sinaloa, ubicada en la costa este del golfo de California. Se

analizaron mapas digitales de diferentes años (1981, 1991, 2004 y 2018) utilizando *softwares* de Sistemas de Información Geográfica (DSAS y CERA) para examinar: a) el desplazamiento y la tasa de cambio en la línea de costa, y b) la vulnerabilidad, las posibles consecuencias y el riesgo de erosión. Los resultados obtenidos indican que entre 1981 y 2018: a) las acciones antrópicas (presas y escolleras) fueron los principales impulsores tanto de los cambios en la línea de costa como del daño ambiental subyacente al riesgo de erosión que se han producido en las últimas décadas; (b) la costa del área de estudio se ha erosionado con un EPR promedio de -3.1 m por año, lo que ha dado lugar a un NSM promedio de -112.9 m, y c) el riesgo de erosión se mantuvo moderado, aunque la vulnerabilidad aumentó de un nivel moderado a un nivel alto y las posibles consecuencias de un nivel muy bajo a uno moderado. Los resultados de este estudio servirán de base para futuros análisis centrados en predecir los cambios en la costa y el riesgo costero.

Palabras clave: erosión costera, DSAS, CERA, riesgo costero, vulnerabilidad, golfo de California.

Received: 14/07/2020

Accepted: 16/08/2021

Tecnología y Ciencias del Agua

OPEN ACCESS

Check for updates

Introduction

Erosion causes shoreline changes at different rates within a timeframe, and its origin can be a response to changes in the infrastructure and climate of coastal areas (*e.g.,* Ahmad & Lakhan, 2012; Ataol, Kale, & Tekkanat, 2019; Fotsi, Pouvreau, Brenon, Onguene, & Etame, 2019; Gómez-Pazo, Pérez-Alberti, & Pérez, 2019; Jonah *et al*., 2016; Kermani, Boutiba, Guendouz, Guettouche, & Khelfani, 2016; Lee, Eom, Do, Kim, & Ryu, 2019). When encountering conditions of vulnerability, coastal erosion is a hazard that represents a source of coastal risk, whose spatial and temporal manifestations have repercussions on other kinds of risk, such as flooding risk (Pollard, Spencer, & Brooks, 2019). According to Escudero-Castillo, Mendoza-Baldwin, Silva-Casarin, Posada-Vanegas, and Arganis-Juaréz (2012), in coastal areas, the meaning of the term "risk" depends on the objective of the study, but most definitions involve vulnerability and hazard; methodologies define the risk in qualitative and/or quantitative terms, and the two approaches on which these methodologies can be based are: (1) a risk analysis approach that combines probabilities and consequences (e.g., Random Shoreface

Tecnología y ciencias del agua, ISSN 2007-2422, 13(6), 249-300. DOI: 10.24850/j-tyca-13-06-06

Translation Model (RanSTM) (Cowell, Roy, & Jones, 1992; Cowell, Roy, & Jones, 1995; Cowell, Thom, Jones, Everts, & Simanovic, 2006; Cowell *et al*., 2016), and (2) a risk assessment approach that evaluates and interprets the perceptions of risk and societal tolerances, and estimates probable future risk, then providing insight into the distribution of risk and its related causes (*e.g.* Coastal Vulnerability Index (CVI) (Thieler & Hammar-Klose, 1999); Coastal Hazard Assessment Module (CHAM) (Viavattene *et al*., 2018). Unfortunately, none of the above-mentioned approaches and methodologies can be used universally. Hence, the selection of a methodology for a particular study area will depend on the required indicators, scale, objectives, and appropriate application scenarios (Narra, Coelho, Sancho, Escudero, & Silva, 2019).

Many of the methodologies mentioned above have been applied at specific sites to generate maps of present and future coastal erosion risk, but without taking into account the evolution of these sites over time or the effects caused by anthropogenic actions (*e.g*., from the last decade to present). This issue does not permit then to learn about the role of key drivers of historical changes and its implications with the coastal risk for a particular site (Stevens, Clarke, Nicholls, & Wadey, 2015). This leads to uncertainty as to whether it is relevant to know the shoreline dynamics in coastal protection and management to promote a planned coastal zone development.

Therefore, this paper aims to analyze the shoreline changes and to assess the coastal erosion risk in different periods for a specific coastal region under interest while applying two state-of-the-art methodologies: the Digital Shoreline Analysis System (DSAS) (Thieler, Himmelstoss, Zichichi, & Ayhan, 2009) and the Coastal Erosion Risk Assessment (CERA; Narra, Coelho, Sancho, & Palalane, 2017).

The authors of this paper believe that the inclusion of the temporal evolution within the framework of coastal erosion risk assessment provides a significant improvement, which, together with the shoreline change analysis results, support the identification of the major driver(s) of the occurred impacts in coastal areas and its relation to erosion risk. In this way, they can provide important elements for coastal protection and management when planning the development of a coastal area.

The study area of this research is the northern coastal strip of the state of Sinaloa, located inside the Gulf of California. Such a coastal zone is subjected to high anthropogenic pressure and possesses, at the same time, considerable biological importance (Enríquez-Andrade *et al*., 2005). In addition, this area is very vulnerable to several coastal hazards like erosion. The selection of such a region is also justified for being an important touristic zone under development (Jiménez-Illescas, Zayas-Esquer, & Espinosa-Carreón, 2019) and for which there is a significant amount of experimental data documented in previous investigations.

Tecnología y Ciencias del Agua

OPEN ACCESS

Check for updates

Study area

The coastal strip under study is approximately 45 km long. It is located on the north coast of the Mexican part of the Pacific Ocean, more precisely in the eastern and lower part of the Gulf of California (see Figure 1). The area essentially consists of three sandy beaches (Macapule, Las Glorias and Bellavista) separated by the mouths of the Sinaloa River and the La Piedra estuary. The relief is flat with a mild slope, and the continental shelf in front of it is, on average, wide and shallow (Kasper-Zubillaga, Carranza-Edwards, & Morales-de-la-Garza, 2007). The astronomical tide is mainly semidiurnal, with spring and neap tidal ranges of 1.2 and 0.5 m, respectively (http://mareografico.unam.mx/). Dominant waves come from the south and southwest sectors, with heights varying between 0.5 and 1.5 m, and periods of 6 to 12 s (Franco-Ochoa, García-Paéz, Plata-Rocha, Montoya-Rodríguez, & Vergara-Sánchez, 2019).

Tecnología y Ciencias del Agua

OPEN ACCESS

Check for updates

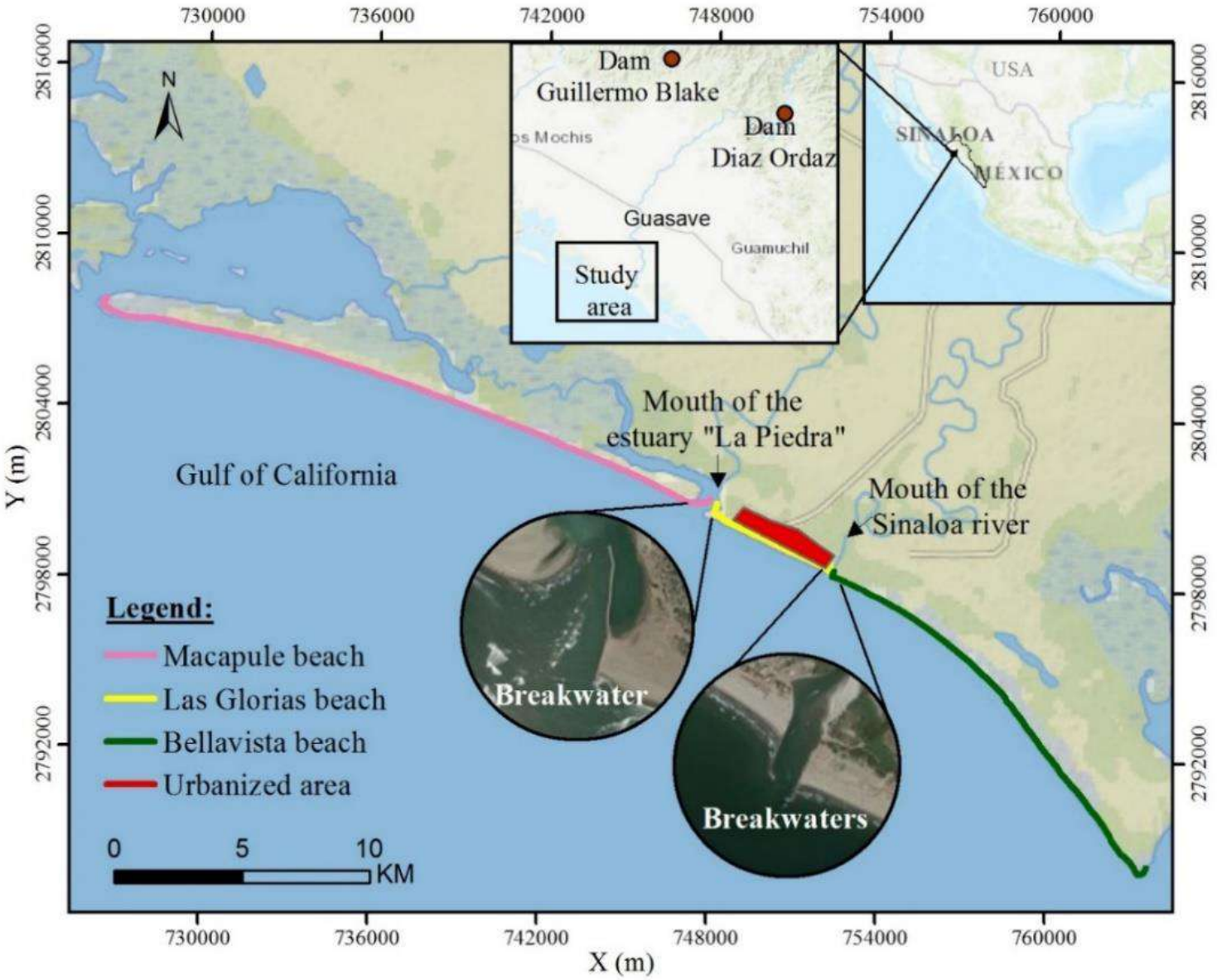

Figure 1. Location of the study area.

It is widely known that in this area, anthropogenic pressures have increased during the last decades, mainly due to the construction of dams and breakwaters, sand extraction, urbanization, etc. In particular, the construction of two dams on the Sinaloa River (1972 and 1981), two breakwaters at its mouth (1992), and another one at the mouth of the estuary La Piedra (2006) has severely affected sediment dynamics. Hence, erosion was felt and has been observed in several points along the coast, principally on Las Glorias beach, thus representing a threat to the coastal ecosystem stability and especially affecting the tourist potential of the region (Jiménez-Illescas *et al*., 2019).

Analyses and methods

For this analysis, it is necessary to rely on the most used indicators for coastal risk assessments, such as tidal and wave data which provide information to evaluate the impacts of the sea on the coast, as well as the variables of distance to the coast, topography, geology, geomorphology, land use, anthropogenic actions and the rate of erosion that allow identifying limits and real changes in the coast. It is also important to

consider socioeconomic data to assess the risk of the population on the coast.

This paper's study period was from 1981 to 2018 and has been divided into three sub-periods (1981 to 1991, 1991 to 2004, and 2004 to 2018) to demonstrate the impact of anthropogenic actions (dams and breakwaters) over time. Shoreline changes were analyzed for every sub-period, and coastal erosion risk was evaluated by applying DSAS and CERA methods, respectively.

The DSAS is an ESRI ArcGIS add-on that calculates rate-of-change statistics for a time series of vector data on the coast (Thieler *et al*., 2009). This analysis can be performed manually, measuring the differences in position between the coastlines of different periods on profiles plotted perpendicular to one of them. For its part, CERA is a complement to QGIS (Quantum GIS Development Team, 2016) proposed by Narra *et al*. (2017), which evaluates the risk of coastal erosion from a qualitative estimate of vulnerability to erosion based on geophysical characteristics of the coastal zone and the potential of erosive agents, and analysis of the consequences of the dangerous event, taking into account the social, environmental, cultural and economic aspects of the territory. The results of these two analyses are combined to obtain the final result sought by CERA to obtain the risk map for coastal erosion.

In addition, and to facilitate the analysis and interpretation of results, the study area was divided into Macapule, Las Glorias, and Bellavista beaches. To clarify every part of the analysis process developed in this research, a comprehensive description of the methodology is described in the following subsections.

Shoreline analysis

Four images are in the Landsat database, as shown in Table 1. Such images were georeferenced to the Universal Transverse Mercator 12 N projection system and WGS84 datum.

Table 1. Satellite images were used in the shoreline analysis.

Satellite and sensor	Date of acquisition
Landsat 2-MSS	Oct-1981
Landsat 5-TM	Oct-1991
Landsat 5-TM	Oct-2004
Landsat 8-OLI	Oct-2018

Then, the position of the shoreline in the images was obtained by locating the line that divides land and sea. This technique for shoreline location is the most used due to its simplicity (Smith & Zartllo, 1990). The images used to find the shoreline location were combinations of infrared bands since they are very useful for detecting the boundary between land and water (Natesan, Parthasarathy, Vishnunath, Kumar, & Ferrer, 2015). In this sense, the best wavelength to discriminate land from pure water is near infrared and middle infrared of 740-2 500 nm (Uysal, Polat, & Aydın, 2018) (see Figure 2).

Tecnología y Ciencias del Agua

OPEN ACCESS

Check for updates

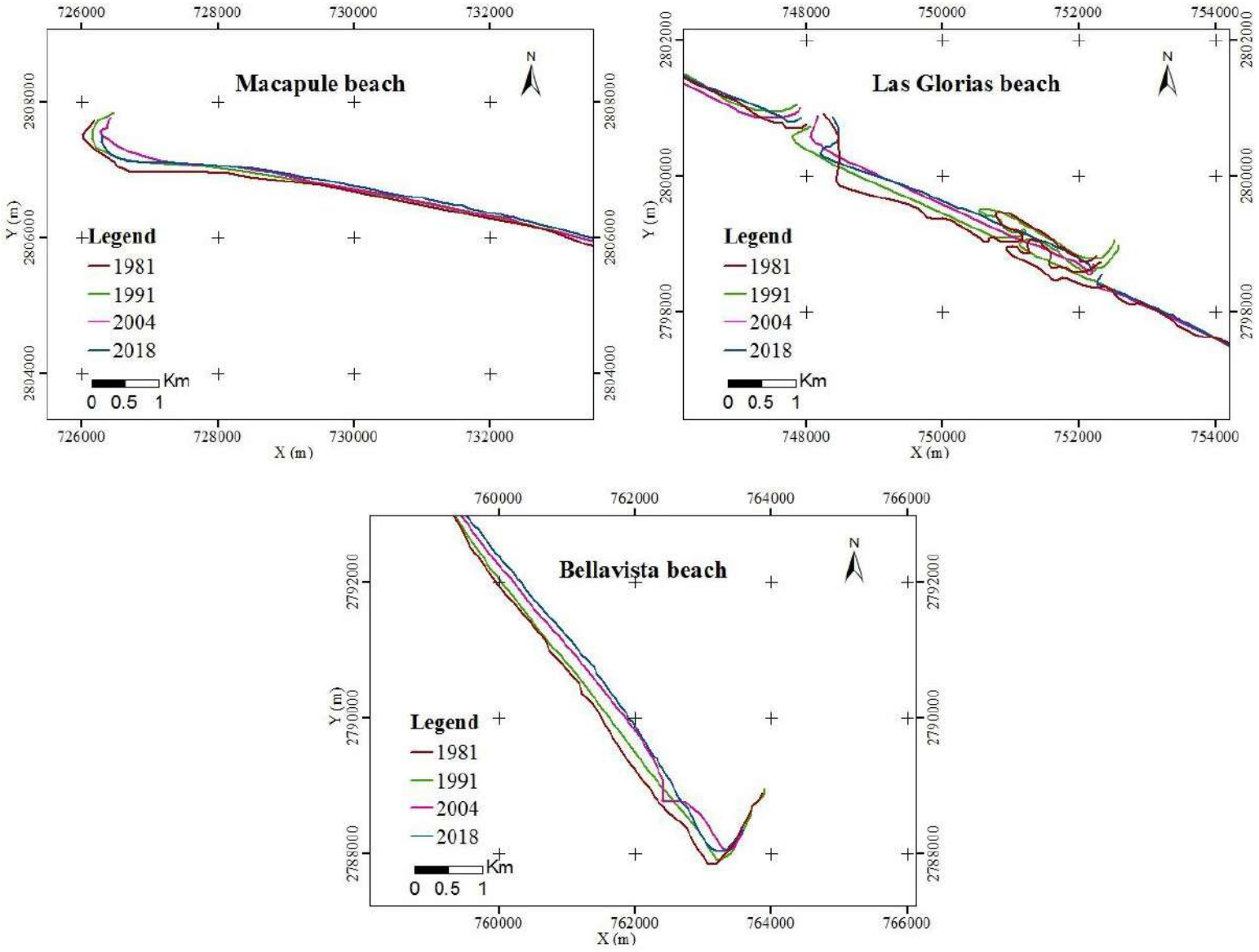

Figure 2. Digitized shoreline of the study area for different years: Macapule (left), Las Glorias (right), and Bellavista (down) beaches.

Moreover, it is important to mention that DSAS also requires a baseline as a starting point for the coastline evolution. This line was generated offshore, parallel to the 1981 shoreline, at a 100 m distance. The number of cross-shore transects was determined following what is reported by Kallepalli, Kakani, and James (2017), who proposed a manual verification of the number of transects given automatically by DSAS. To measure changes in the shoreline of the study area, statistical measurements of the Net Shoreline Movement (NSM) were calculated, which is the distance between the oldest and youngest shorelines. In addition, the End Point Rate (EPR) was extracted, which is obtained by dividing the distance between shorelines concerning the number of years that have elapsed. Then, from this EPR, areas of very high, high, low, and low erosion or accretion were determined.

Coastal risk assessment

As previously mentioned, the coastal risk assessment was performed by CERA. It requires georeferenced digital maps considering the following 13 parameters, which are generally known as indicator maps:

1. Distance to the shoreline.
2. Topography.
3. Geology.
4. Geomorphology.
5. Ground cover.
6. Anthropogenic actions.
7. Maximum significant wave height.
8. Maximum tidal range.
9. Shoreline change rate.
10. Population density.
11. Economy.
12. Ecology.
13. Heritage.

The data were cut inland, thus covering a 2 km wide coastal strip. The established Coordinate Reference System (CRS) was WGS84 / UTM zone 12N (EPSG: 32612) for all the maps, which conglomerates the database.

All the maps were built from the direct transformation of original data; then, raster maps were classified, from 1 to 5, according to the characteristics of every parameter along the entire study area (see Table B1 in Supplementary materials).

Classification 1 corresponds to the lowest severity, and an increase in classification indicates a growing severity level. Maps 1 to 9 are used to assess the vulnerability; the weight of each parameter may change with increasing distance to the shoreline. While maps 10 to 13 are used to assess the potential consequences, in this case, all the parameters have the same weight. Then, using the vulnerability and potential consequences maps, the coastal risk to erosion map was obtained using a raster calculator. The vulnerability, potential consequences, and risk maps were also classified by severity levels from 1 to 5 for all the study areas. The criteria, tables, equations for quantifying the weight of each parameter, and classified maps are documented in Narra *et al*. (2017).

In summary, in this paper, the Global Classification (GC) of parameters was evaluated by a weighted average as follows:

$$GC = \frac{\sum A * Cl}{100} \quad (1)$$

Where *GC* is an overall classification dimensional parameter; A represents the area occupied by the class level (1 to 5) as a percentage, and Cl is the class level. The value of *GC* equal to one corresponds to a very low level, and increasing values of *GC* indicate increasing severity, up to a maximum of 5 (very high level).

Results

The results of the shoreline analysis with DSAS led to the identification of coastal erosion hotspots along the coast of the study area (see Figure 3 and Figure 4). Erosion has been concentrated on Las Glorias beach and on the SE margin of Bellavista beach, and more recently on the SE margin of Macapule beach (mouth of the estuary "La Piedra").

Tecnología y Ciencias del Agua

OPEN ACCESS

Check for updates

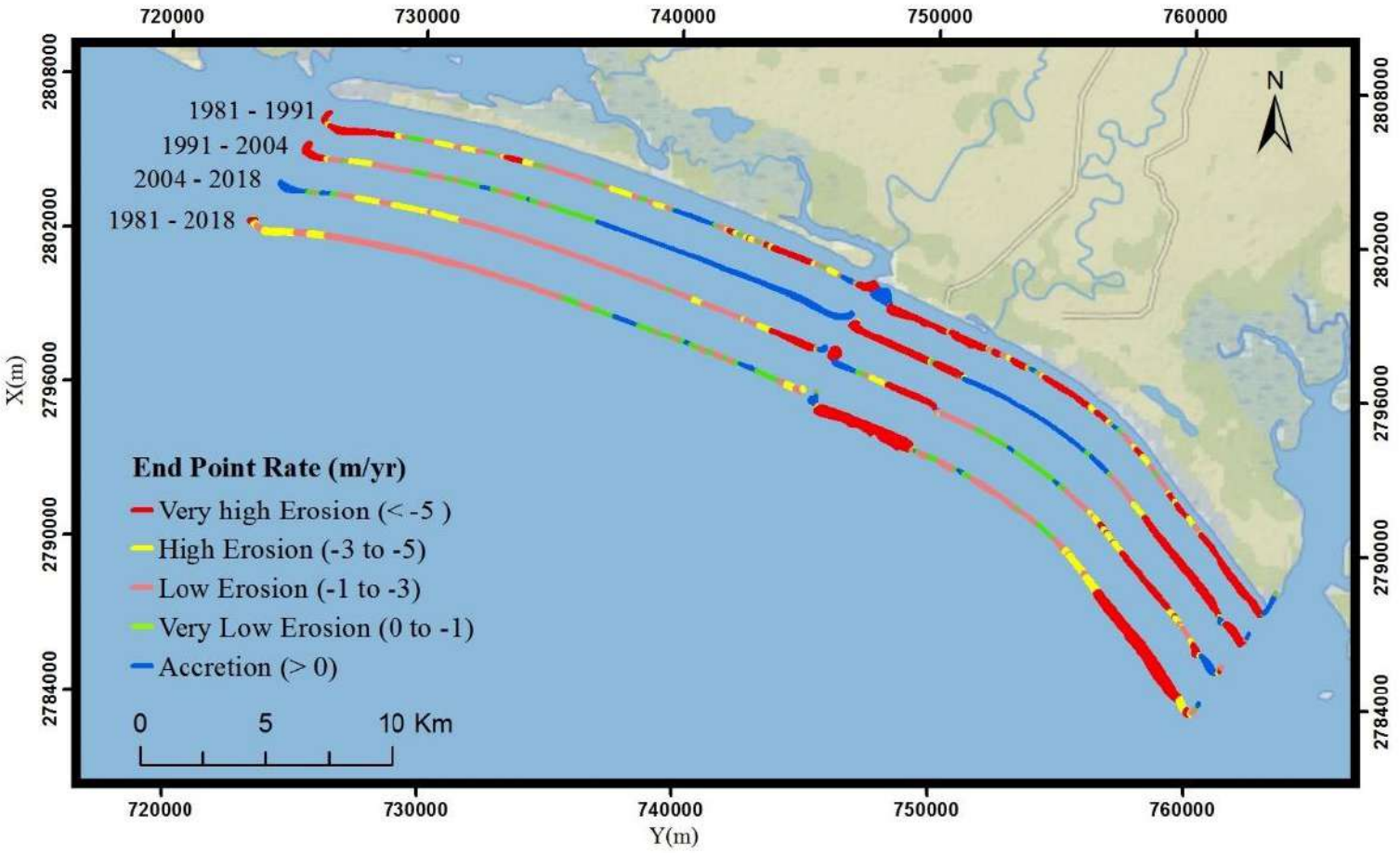

Figure 3. End Point Rate (EPR) along the study area for all periods.

Tecnología y Ciencias del Agua

OPEN ACCESS

Check for updates

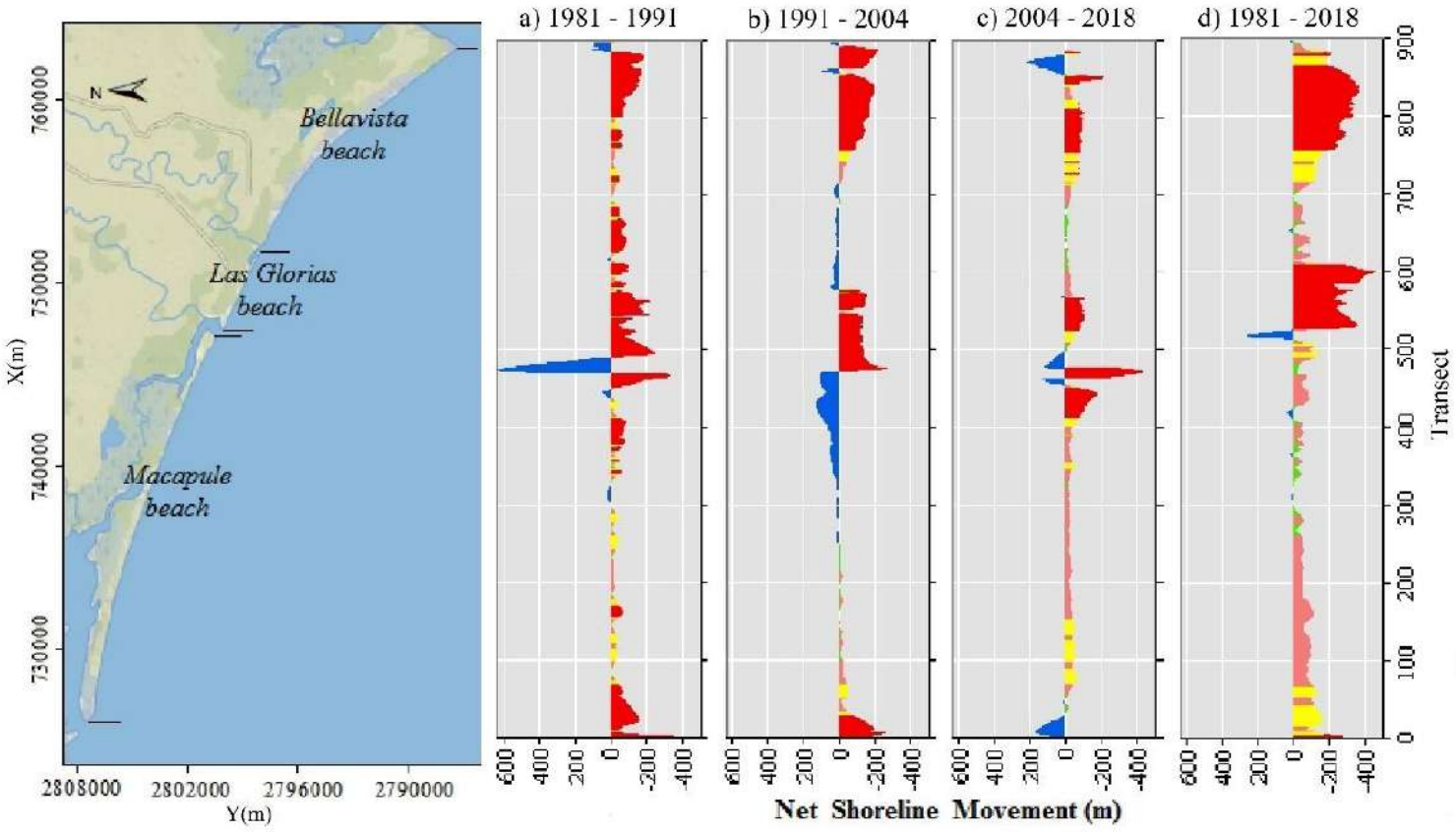

Figure 4. Net Shoreline Movement (NSM) along the study area for all periods.

On the other hand, when analyzing the indicator maps of vulnerability and potential consequences for each year (see Appendix A and Figures A1 to A4 in Supplementary materials), it was observed that six parameters of vulnerability (distance to shoreline, topography,

geology, geomorphology, maximum significant wave height, and maximum tidal range) have not varied throughout the whole study period (1981 to 2018). Only the parameters of ground cover, anthropogenic actions, shoreline change rate, and parameters of consequences (population density, economy, ecology, and heritage) have been varying at least once during any of the study sub-periods.

Figure 5 shows the vulnerability, potential consequences, and risk maps obtained with CERA (see Appendix B in Supplementary materials), where the spatial distribution over time of these parameters in the study area can be seen at first sight.

Tecnología y Ciencias del Agua

OPEN ACCESS

Check for updates

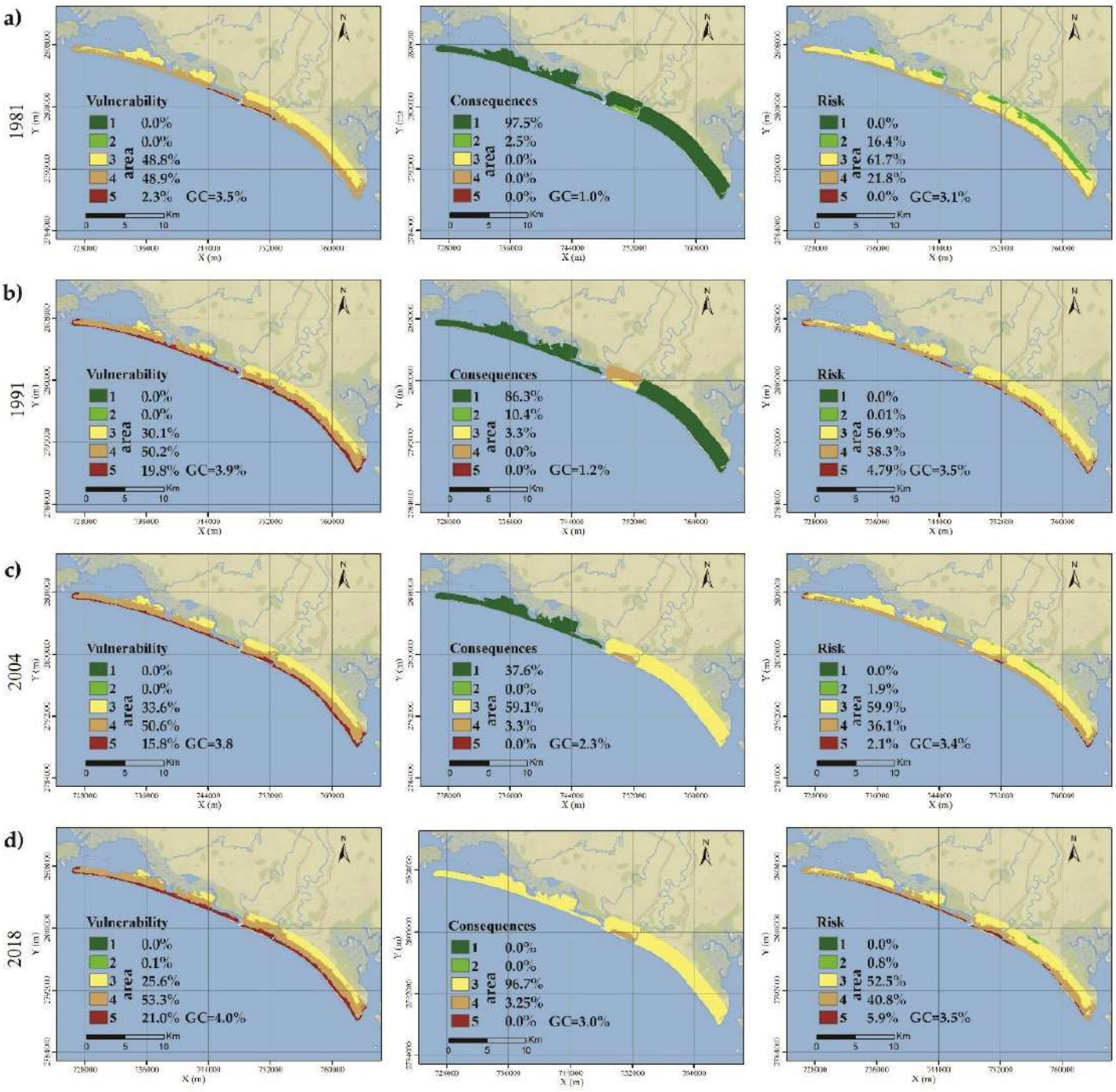

Figure 5. Vulnerability, potential consequences, and risk maps for the study area.

The following subsections present the results of the shoreline analysis and erosion risk assessment for each sub-period.

Sub-period 1981 to 1991

Throughout this ten-year sub-period, the main anthropogenic actions identified were the construction of the Guillermo Blake Aguilar and Gustavo Díaz Ordaz dams on the Sinaloa River. During such a period, the entire Las Glorias beach experienced an average EPR of -13.4 m per year, which caused an average NSM of -127.6 m. Simultaneously, Bellavista and Macapule nearby beaches mainly experienced erosion problems, with an average NSM of -67.4 m and -41.0 m, respectively. The average EPR of these beaches was -7.3 m per year for Bellavista and -4.4 m per year for Macapule (see Table 2).

Table 2. Evolution rates for the sub-period 1981-1991.

Variable	Total area	Macapule beach	Las Glorias beach	Bellavista beach
Average EPR (m/year)	-5.04	-4.4	-13.4	-7.3
Average NSM (m)	-46.8	-41.0	-127.6	-67.4

After analyzing risk assessment results for this sub-period (see Figure 5, a-b), it can be observed that the average EPR (-5.04 m per year) induced by anthropogenic actions has increased the vulnerability GC from 3.5 to 3.9 (+0.4). On the other hand, population, economy, and patrimony have increased the consequences GC from 1.0 to 1.2 (+0.2). This finally caused the risk GC to increase from 3.1 to 3.5 (+0.4).

Sub-period 1991 to 2004

During the second sub-period, from 1991 to 2004 (13 years), the construction of two breakwaters at the mouth of the Sinaloa River, for the first time in the study area, interrupted the net longshore sediment transport from southeast to northwest. As a result, this modified the average EPR of Las Glorias beach to -9.3 m per year, which led to an average NSM of -127.7 m over this period and promoted accumulation on Bellavista beach on its NW margin while the SE margin continued to erode. In general, Bellavista beach experienced an average NSM of -57.6 m at an average EPR of -4.2 m per year. In this sub-period and in contrast to the previous one, Macapule beach mainly experienced accumulation, and only its NW margin kept eroding. Its average NSM was 5.05 m at an average EPR of 0.4 m per year (see Table 3).

Table 3. Evolution rates for the sub-period 1991-2004.

Variable	Total area	Macapule beach	Las Glorias beach	Bellavista beach
Average EPR (m/year)	-2.4	0.4	-9.3	-4.2
Average NSM (m)	-32.9	5.05	-127.7	-57.6

The risk assessment results for this sub-period (see Figure 5, b-c) showed that mainly due to the reduction in the average EPR (from -5.04 m to -2.4 m per year), the vulnerability GC has decreased from 3.5 to 3.4 (-0.1), in contrast to the consequences GC that has increased from 1.2 to 2.3 (+1.1) because of a growing economy. This caused the risk GC to decrease from 3.5 to 3.4 (-0.1).

Sub-period 2004 to 2018

During the sub-period of 2004 – 2018 (14 years), for a second time in the study area, the net longshore sediment transport from southeast to northwest was interrupted by the construction of another breakwater structure on Las Glorias beach. This anthropogenic action promoted accumulation on the NW margin of that beach while the SE margin continued to erode. Although it did not affect Bellavista beach, it generated erosion on the Macapule beach SE margin. During this sub-period, Las Glorias, Bellavista, and Macapule beaches experienced NSM averages of -75.9 m, -30.2 m, and -27.8 m at EPR averages of -5.4 m, -2.2 m, and -1.9 m per year, respectively (see Table 4).

Table 4. Evolution rates for the sub-period 2004-2018.

Variable	Total area	Macapule beach	Las Glorias beach	Bellavista beach
Average EPR (m/year)	-2.5	-1.9	-5.4	-2.2
Average NSM (m)	-34.3	-27.8	-75.9	-30.2

In this sub-period, risk assessment results (see Figure 5, c-d) demonstrated that the vulnerability GC has increased from 3.8 to 4.0 (+0.2) due to an increase in the average EPR (from -2.4 m to -2.5 m per year). Also, the consequences GC has increased from 2.3 to 3.0 (+0.7) due to an increase in the ecological value of the region due to the declaration of Macapule beach as a protected coastal area. Thus, the risk GC has increased from 3.4 to 3.5 (+0.1).

Discussion

The results of this research demonstrated that between 1981 and 2018, the study area's average EPR value was -3.1 m per year, leading to an average NSM of -112.9 m. Then, it can be stated that the most erosive beach is Las Glorias, with an average NSM of -235.9 m at an average EPR of -6.4 m per year, and the least erosive is Macapule, with an average NSM of -61.6 m at an average EPR of -1.6 m per year. On the other side, Bellavista beach experienced an average NSM of -148.2 m at an average EPR of -4.0 m per year (see Table 5).

Table 5. Evolution rates for the sub-period 1981-2018.

Variable	Total area	Macapule beach	Las Glorias beach	Bellavista beach
Average EPR (m/year)	-3.1	-1.6	-6.4	-4.0
Average NSM (m)	-112.9	-61.6	-235.9	-148.2

The vulnerability GC has then increased from 3.5 to 4.0 (+0.5), *i.e.,* from a moderate to a high level. This was due to the changes in ground cover, anthropogenic actions, and the shoreline change rate. Similarly, the potential consequences of GC have increased from 1.0 to 3.0 (+2.0), an increment from a very low to a moderate level, resulting from an increase in population density, economy, ecology, and heritage. Regarding the risk GC, it has only increased from 3.1 to 3.5 (+0.4), which means that the risk level remained moderate (see Figure 5, a-d).

The most plausible explanation for the differences in the NSM and EPR along the shoreline may be found in the type of coastline evolution that occurred meanwhile, with the different anthropogenic actions like the damming of the Sinaloa River and the construction of breakwaters transversely to the shoreline. In agreement with earlier analyses in the study area (*e.g.,* Alcántar, 2007; Jiménez-Illescas *et al*., 2019), the results of this work indicate that anthropogenic actions (dams and breakwaters) are the main drivers of changes that have occurred in recent decades on the shoreline. Infrastructure such as dams and breakwaters is one of the two main drivers linked to the modern dynamics of the shoreline, according to Gómez-Pazo *et al*. (2019), the other one being urbanization. In the study area, urbanization throughout the study period has been concentrated at Las Glorias beach. However, the degree of urbanization does not seem to affect the sediment dynamics as observed on other coasts, for example, at Chachalacas beach inside the Gulf of

Mexico, where urban development has been taking place along the coast, and coastal squeeze is increasing (Martínez, Landgrave, Silva, & Hesp, 2019).

The most important erosion in the study area occurred in the sub-period 1981-1991, during which the shoreline suffered an average NSM of -57.6 m at an average EPR of -4.2 m per year. Certainly, the damming of the Sinaloa River reduced the sediment load reaching the coast. This has caused alterations in the shoreline, which can still be felt after several years (Ataol *et al*., 2019). Like this study, the dam erosion inside the Gulf of California has been documented by Ezcurra *et al*. (2019) for the coastline located around the El Fuerte and Santiago rivers. When these rivers were dammed, the shoreline experienced a rapid recession in what should otherwise have been an accretional area.

During the sub-period of 1991 to 2004, the erosion dynamics mainly affected Las Glorias beach and the SE margin of Bellavista beach. The net longshore sediment transport from southeast to northwest eroded the SE margin of Bellavista beach. The material from this erosion was deposited in the updrift side of the breakwater of the mouth of the Sinaloa River, which generated erosion on Las Glorias beach. For its part, Macapule beach experienced accretion in general terms, which is perhaps due to the deposition of sediment issued from the erosion of Las Glorias beach,

since when there is erosion on one beach, there is deposition in another one, near or far away (Pollard *et al*., 2019).

In the sub-period of 2004 to 2018, it is important to note that the downdrift erosion, caused by the breakwater of the NW margin of Las Glorias beach, modified the mouth of the estuary "La Piedra." Furthermore, it is possible that the mouth will continue to enlarge and generate more erosion on the SE margin of Macapule beach. A situation similar to the above-described has also been observed at Chachalacas beach (Martínez *et al*., 2019), where the construction of breakwaters is affecting the stability of the beach and the mouth of the Actopan River. The shoreline has changed rapidly and does not seem to have been stabilized yet, which evidences the need to monitor it to avoid potentially drastic changes in Chachalacas beach. In the study area of this research, the mouth of the estuary "La Piedra" needs to be regularly monitored as well since the results obtained indicate that the construction of the breakwater on the NW margin of Las Glorias beach has had a considerable effect on the evolution of the SE margin of Macapule beach.

On the other hand, the erosion risk has changed over the study period due to changes in ground cover, anthropogenic actions, shoreline change rate, population density, economy, ecology, and heritage. The results indicate that anthropogenic actions and induced erosion are the main drivers of environmental damage underlying the erosion risk.

According to Stevens *et al*. (2015), these drivers can change over time. A full analysis should include an evaluation of how these drivers have historically evolved and how they are prone to evolve in the future. Therefore, the results of this study provide a basis for future investigations focused on predicting shoreline changes and coastal risk via scenario analyses. However, these results should be considered with caution, as they are still subject to uncertainties and largely depend on the ranges of values in Table B1 proposed by Narra *et al*. (2017) and on the quality of field data for the site-specific parameters used as input data.

Conclusions

The main conclusion of this study is that the two dams on the Sinaloa River (constructed in 1972 and 1981, respectively) and two breakwaters built at the Sinaloa River mouth (1992) and the mouth of the estuary "La Piedra" (2006), are the main drivers of both the shoreline changes and environmental damage, then underlying the erosion risk that has

incremented in recent decades on the northern coastal strip of the state of Sinaloa.

Between 1981 and 2018, the coastline of the study area has been eroding with an average EPR of -3.1 m per year that led to an average NSM of -112.9 m, being Las Glorias beach the most eroded one with an average NSM of -235.9 m at an average EPR of -6.4 m per year. The most significant erosion in the entire coast of the study area occurred during the sub-period 1981 to 1991 due to the damming of the Sinaloa River, which reduced the sediment load reaching the coast. In the other sub-periods (1991 to 2004 and 2004 to 2018), the interruption of net longshore sediment transport from southeast to northwest caused by breakwaters mainly affected Las Glorias beach and the mouth of the La Piedra estuary. The latter needs to be monitored to avoid potentially drastic changes in the SE margin of Macapule beach. On the other hand, the risk level remained moderate, although it increased by 0.5 units in its GC parameter. Finally, the vulnerability and potential consequences GCs increased from a moderate to a high level and from a very low to a moderate level of severity, respectively.

A GIS database was generated, which includes statistical data, thematic maps, and linked indices from which the results were obtained, and which will be useful for future studies focused on predicting shoreline changes and coastal risk.

Tecnología y Ciencias del Agua

OPEN ACCESS

Check for updates

Supplementary materials

Appendix A. Gathering and processing data for the maps

To generate the topographic map of the study area, the Mexican Elevation Continuum (MEC) database from the National Institute of Geography and Statistics (INEGI, by its initials in Spanish) was used. This data set represents the elevations of the Mexican continental territory, with a resolution of 15 m. It is georeferenced by the system ITRF92 and was published in 2013. The extraction of the study area from the MEC was carried out with ArcGis tools. The geological maps were based on GLiM (Global lithological map) and INEGI geospatial information from geological data. Similarly, the geomorphological and land cover maps were made based on INEGI geospatial information from physiographic,

land, and vegetation data. For the map of anthropogenic actions, satellite images were used, where coastal defense structures and changes in the shoreline were identified to infer if there were sedimentary sources nearby.

The map of maximum significant wave height was made based on the deep-water wave reanalysis database of node PAC17MX from the Mexican Oceanic Wave Atlas (ATLOOM, by its initials in Spanish), developed by the Mexican Institute of Transportation (IMT, by its initials in Spanish) (Montoya-Rodríguez, 2016). Regarding creating the maximum tidal range map, the Secretary of Navy provided the data (SEMAR, by its initials in Spanish), which were taken from the Topolobampo Mareographic Station. Then, in this paper, the average wave height during storm conditions and the average range of spring tides were considered as the maximum significant wave height and maximum tidal range, respectively. During the generation of these maps, the parameters mentioned above were evaluated as a single value for the entire study area. The shoreline change rate map was generated with a shoreline analysis from satellite images using DSAS as described in the subsection Shoreline analysis. For the creation of the shoreline change rate map away from the coast, the shoreline 2018 was considered the basis line.

The information required for the population density and economic parameters was also obtained from INEGI's database corresponding to the 2010 National Census. The data used to generate the ecology map considered protected areas defined by the National Commission for the Knowledge and Use of Biodiversity (Conabio, by its initials in Spanish) and the National Commission on Protected Areas (Conanp, by its initials in Spanish). The heritage map was calculated by visual analysis of satellite images identifying whether there were continuous or discontinuous urban areas, roads, and historical or important monuments near the coast.

Digital maps (sourced from Arcgis®, Environmental Systems Research Institute) for the years 1981, 1991, 2004, and 2018 are presented in Figure A1, Figure A2, Figure A4, and Figure A4.

Tecnología y Ciencias del Agua

OPEN ACCESS

Check for updates

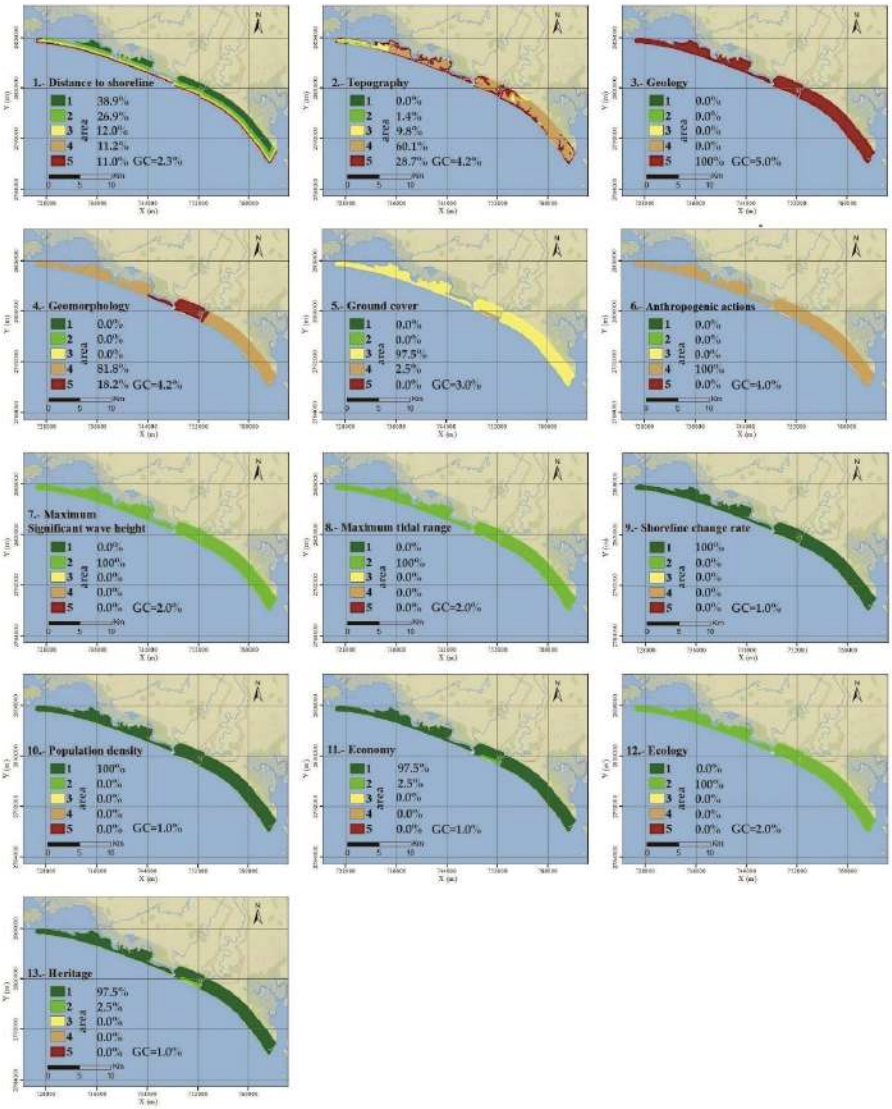

Figure A1. Indicator maps of vulnerability (1 to 9) and potential consequences (10 to 13) of 1981.

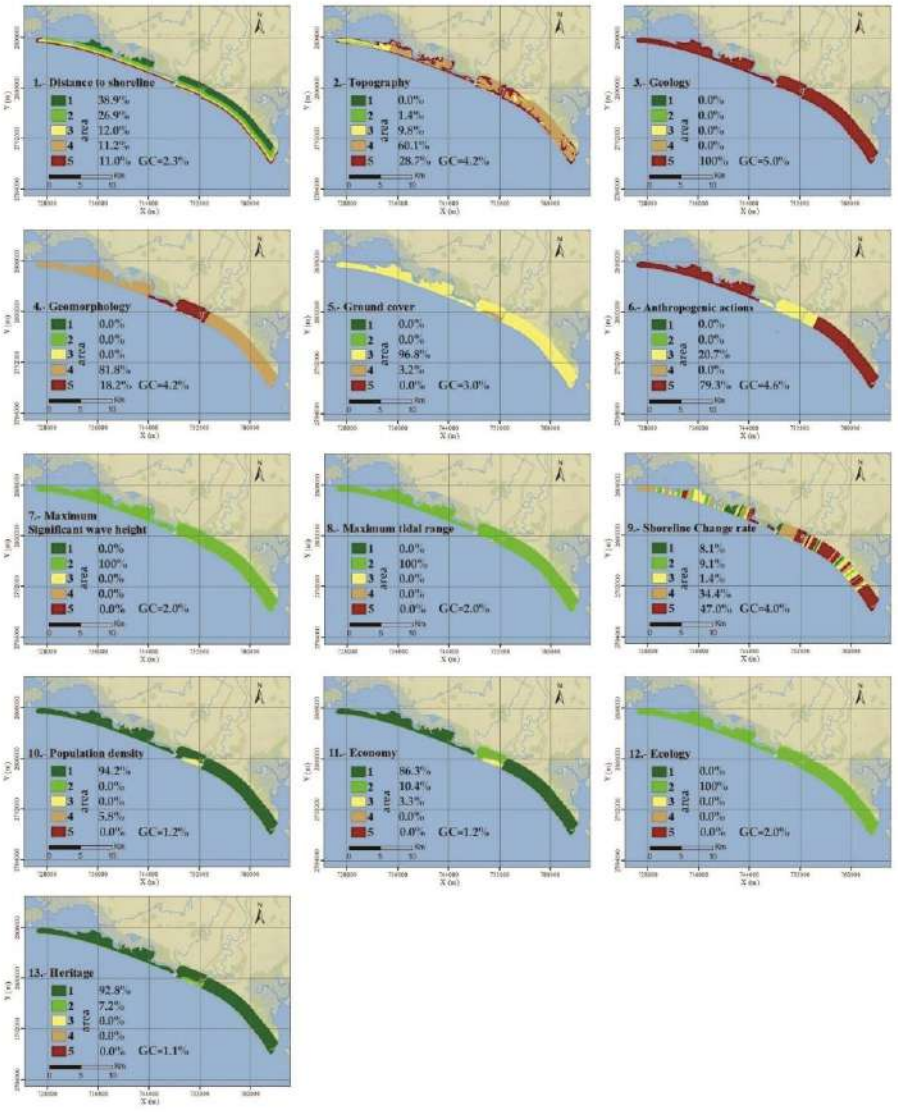

Figure A2. Indicator maps of vulnerability (1 to 9) and potential consequences (10 to 13) of 1991.

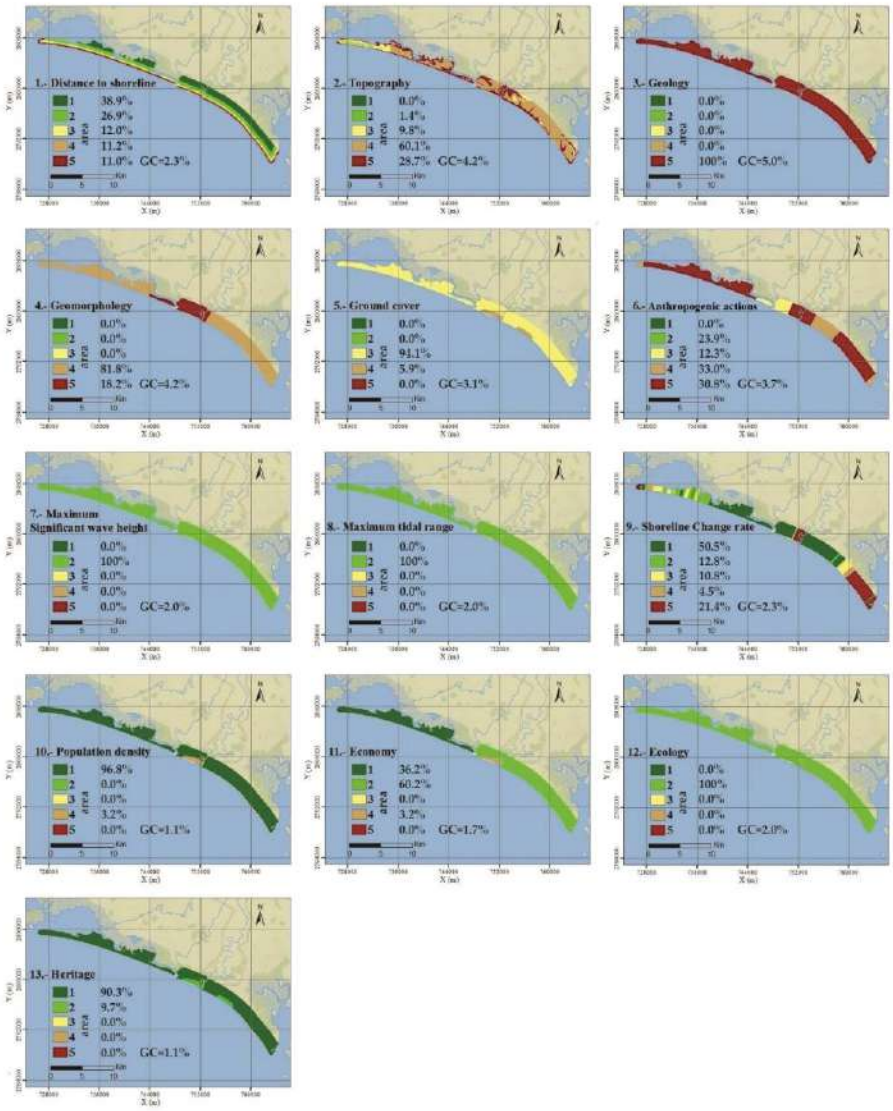

Figure A3. Indicator maps of vulnerability (1 to 9) and potential consequences (10 to 13) of 2004.

Tecnología y Ciencias del Agua

OPEN ACCESS

Check for updates

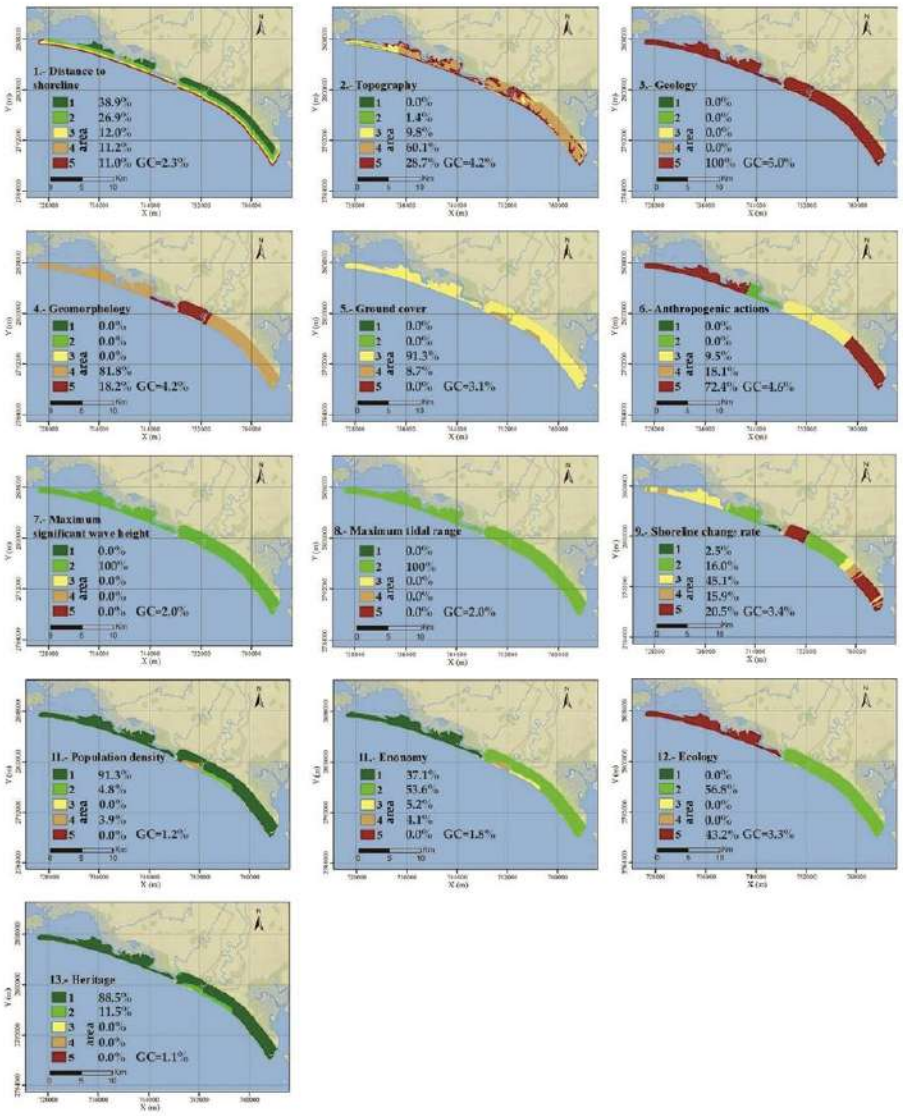

Figure A4. Indicator maps of vulnerability (1 to 9) and potential consequences (10 to 13) of 2018.

Tecnología y Ciencias del Agua

OPEN ACCESS

Check for updates

Appendix B. Application of the CERA methodology

The CERA method required data processing to create indicator maps (the processing of each of them is described in Appendix A), which were obtained from the direct transformation of original data getting raster maps classified from 1 to 5. The five levels for classifying the indicator maps needed to run the CERA application are presented in Table B1. Each of the indicator maps was generated with an output resolution of 5 m/px based on what was indicated by the author of CERA, which performed various tests and concluded that this is the most acceptable resolution because it provides a reasonable calculation time without compromising the detail of the data of any other indicator map, for this reason, all indicator maps were created in this resolution (Table B1).

Table B1. Classification of parameters, adapted from Narra *et al*. (2017).

Parameters	Very low	Low	Moderate	High	Very high

	1	2	3	4	5
Distance to the shoreline (m)	>1000	[500,1 000]	[300,500]	[150,300]	≤ 150
Topography (m)	>30	[20,30]	[10,20]	[5,10]	≤ 5
Geology	Magmatic rocks	Metamorphic rocks	Sedimentary rocks	Non-consolidated coarse sediments	Non-consolidated fine sediments
Geomorphology	Mountains	Rock cliffs	Erosive cliffs; sheltered beaches; dunes	Exposed beaches; coastal plains	River mouths; estuaries
Ground cover	Forest	Vegetation cultivated	Non-covered	Rural urbanized	Urbanized; industrial
Anthropogenic actions	Shoreline stabilization intervention	Intervention without sediment sources reduction	Intervention with sediment sources reduction	Without interventions or sediment sources reduction	Without intervention and with sediment sources reduction
Maximum significant wave height (m)	<3.0	[3.0,5.0]	[5.0,6.0]	[6.0,6.9]	≥ 6.9

Maximum tidal range (m)	<1.0	[1.0,2.0]	[2.0,4.0]	[4.0,6.0]	≥ 6.0
Average erosion/accretion rates (m/year)	>0.0 Accretion	[0.0, -1.0] Erosion	[-1.0, -3.0] Erosion	[-3.0, -5.0] Erosion	≤ -5.0 Erosion
Population density (inhabitant/km^2)	<125	[125,250]	[250,500]	[500,1 000]	≥ 1000
Economy (number of employments)	0	[0,120]	[120,240]	[240,480]	>480
Ecology	No ecological relevance	Agricultural reserve; areas of community interest	Ecological protected area	Coastal protection zone	Natural reserve
Heritage	No heritage	Scattered houses; roads	Urban settlements	Regional historic buildings; critical facilities	National monuments

The information obtained for the generation of the indicator maps to assess vulnerability was based on current and historical data, as required by each parameter. The nine parameters for calculating coastal

vulnerability are distance to the coast (shortest linear distance from any point on land to the coast), topography, geology, geomorphology, land cover, anthropogenic actions, significant maximum wave height (within a representative data period), maximum tidal range and erosion/accretion rate, which are attributed a classification from 1 to 5 based on Table B1. The vulnerability at each point is calculated by calculating the weighted average of the weights of the nine parameters based on what is established by Narra *et al*. (2017).

The calculation of the consequences is similar to that of vulnerability but includes only four parameters: population density, economy, ecology, and heritage. In the same way, these parameters are classified from 1 to 5 based on Table B1. This map was obtained from the average of the four maps with the same weight.

The vulnerability and consequence maps are combined using the risk matrix presented in Figure B1 to obtain the coastal erosion risk map.

		Consequence				
		I	II	III	IV	V
Vulnerability	I	I	I	I Very low	II	III
	II	I	II	II Low	III	IV
	III	I	II	III Moderate	IV	V
	IV	II	III	IV High	IV	V
	V	III	IV	V Very high	V	V

Figure B1. Risk matrix used by CERA (Narra *et al*., 2017).

Risk is defined in 5 different classes: "I" represents very low risk, and "V" is very high risk. The risk matrix is symmetric, considering both vulnerability and consequence equally important (Narra *et al*., 2017).

Acknowledgments

The authors wish to thank the Mexican Institute of Transportation (IMT, by its initials in Spanish) and the Ministry of the Navy (SEMAR, by its initials in Spanish) for the information provided in the preparation of this

paper. The authors are also very grateful to Dr. Sébastien de Brye for his helpful and unselfish support in reviewing this paper. This research was funded by the Autonomous University of Sinaloa under research grant number PROFAPI2022/A1_016.

References

Ahmad, S. R., & Lakhan, V. C. (2012). GIS-based analysis and modeling of coastline advance and retreat along the coast of Guyana. *Marine Geodesy*, 35(1), 1-15. Recovered from https://doi.org/10.1080/01490419.2011.637851

Alcántar, R. (2007). *Temporal space variability of the beach profile, in "Las Glorias" beach (Master's degree).* Guasave, Mexico: National Polytechnic Institute.

Ataol, M., Kale, M. M., & Tekkanat, İ. S. (2019). Assessment of the changes in shoreline using digital shoreline analysis system: A case study of Kızılırmak Delta in northern Turkey from 1951 to 2017. *Environmental Earth Sciences*, 78(19), 1-9. Recovered from https://doi.org/10.1007/s12665-019-8591-7

Cowell, P. J., Roy, P. S., & Jones, R. A. (1992). Shoreface translation model: Computer simulation of coastal-sand-body response to sea level rise. *Mathematics and Computers in Simulation*, 33(5-6), 603-

608. Recovered from https://doi.org/10.1016/0378-4754(92)90158-D

Cowell, P. J., Roy, P. S., & Jones, R. A. (1995). Simulation of large-scale coastal change using a morphological behavior model. *Marine Geology*, 126(1-4), 45-61. Recovered from https://doi.org/10.1016/0025-3227(95)00065-7

Cowell, P. J., Thom, B. G., Jones, R. A., Everts, C. H., & Simanovic, D. (2006). Management of uncertainty in predicting climate-change impacts on beaches. *Journal of Coastal Research*, 221(221), 232-245. Recovered from https://doi.org/10.2112/05a-0018.1

Cowell, P. J., Stive, M. J. F., Niedoroda, A. W., Vriend, H. J. De, D. J., Swift, P., & Capobianco, M. (2016). The coastal-tract (Part 1): A conceptual approach to aggregated modeling of low-order coastal change stable. *Journal of Coastal Research*, 4(19), 812-827.

Enríquez-Andrade, R., Anaya-Reyna, G., Barrera-Guevara, J. C., De-los Ángeles-Carvajal-Moreno, M., Martínez-Delgado, M. E., Vaca-Rodríguez, J., & Valdés-Casillas, C. (2005). An analysis of critical areas for biodiversity conservation in the Gulf of California Region. *Ocean and Coastal Management*, 48(1), 31-50. Recovered from https://doi.org/10.1016/j.ocecoaman.2004.11.002

Escudero-Castillo, M., Mendoza-Baldwin, E., Silva-Casarin, R., Posada-Vanegas, G., & Arganis-Juaréz, M. (2012). Characterization of risks

in coastal zones: A review. *Clean-Soil, Air, Water*, 40(9), 894-905. Recovered from https://doi.org/10.1002/clen.201100679

Ezcurra, E., Barrios, E., Ezcurra, P., Ezcurra, A., Vanderplank, S., Vidal, O., & Aburto-Oropeza, O. (2019). A natural experiment reveals the impact of hydroelectric dams on the estuaries of tropical rivers. *Science Advances*, 5(3). Recovered from https://doi.org/10.1126/sciadv.aau9875

Fotsi, Y. F., Pouvreau, N., Brenon, I., Onguene, R., & Etame, J. (2019). Temporal (1948-2012) and dynamic evolution of the Wouri estuary coastline within the gulf of Guinea. *Journal of Marine Science and Engineering*, 7(10). Recovered from https://doi.org/10.3390/jmse7100343

Franco-Ochoa, C., García-Paéz, F., Plata-Rocha, W., Montoya-Rodríguez, J. M., & Vergara-Sánchez, M. Á. (2019). Observation and analysis of hydro-morphologic parameters in Las Glorias beach, Mexico. *Tecnología y Ciencias del Agua*, 10(2), 153-170. Recovered from https://doi.org/10.24850/j-tyca-2019-02-06

Gómez-Pazo, A., Pérez-Alberti, A., & Pérez, X. L. O. (2019). Recent evolution (1956-2017) of rodas beach on the Cíes Islands, Galicia, NW Spain. *Journal of Marine Science and Engineering*, 7(5). Recovered from https://doi.org/10.3390/jmse7050125

Jiménez-Illescas, Á. R., Zayas-Esquer, M. M., & Espinosa-Carreón, T. L. (2019). Integral management of the coastal zone to solve the problems of erosion in Las Glorias Beach, Guasave, Sinaloa, Mexico. In: *Coastal Management* (pp. 141-163). Recovered from https://doi.org/10.1016/B978-0-12-810473-6.00010-8

Jonah, F. E., Boateng, I., Osman, A., Shimba, M. J., Mensah, E. A., Adu-Boahen, K., & Effah, E. (2016). Shoreline change analysis using end point rate and net shoreline movement statistics: An application to Elmina, Cape Coast and Moree section of Ghana's coast. *Regional Studies in Marine Science*, 7, 19-31. Recovered from https://doi.org/10.1016/j.rsma.2016.05.003

Kallepalli, A., Kakani, N. R., & James, D. B. (2017). Digital shoreline analysis system-based change detection along the highly eroding Krishna–Godavari delta front. *Journal of Applied Remote Sensing*, 11(03), 1. Recovered from https://doi.org/10.1117/1.jrs.11.036018

Kasper-Zubillaga, J. J., Carranza-Edwards, A., & Morales-de-la-Garza, E. (2007). Textural characterization of beach sands from the Gulf of California, Mexico: Implications for coastal processes and relief. *Ciencias Marinas*, 33(1), 83-94. Recovered from https://doi.org/10.7773/cm.v33i1.1018

Kermani, S., Boutiba, M., Guendouz, M., Guettouche, M. S., & Khelfani, D. (2016). Detection and analysis of shoreline changes using geospatial tools and automatic computation: Case of jijelian sandy coast (East Algeria). *Ocean and Coastal Management*, 132, 46-58. Recovered from https://doi.org/10.1016/j.ocecoaman.2016.08.010

Lee, Y., Eom, J., Do, J., Kim, B., & Ryu, J. (2019). Shoreline movement monitoring and geomorphologic changes of beaches using lidar and UAVs images on the coast of the East Sea, Korea. *Journal of Coastal Research*, (90), 409-414. Recovered from https://doi.org/10.2112/SI90-052.1

Martínez, M. L., Landgrave, R., Silva, R., & Hesp, P. (2019). Shoreline dynamics and coastal dune stabilization in response to changes in infrastructure and climate. *Journal of Coastal Research*, 92(sp1), 6. Recovered from https://doi.org/10.2112/si92-002.1

Montoya-Rodríguez, J. M. (2016). Red Nacional de Datos Oceanográficos para Zonas Costeras. *Journal of Civil Engineering (IC, by Its Initials in Spanish)*, 566, 14-18. Recovered from https://issuu.com/helios_comunicacion/docs/ic-566_ok/16

Narra, P., Coelho, C., Sancho, F., Escudero, M., & Silva, R. (2019). Coastal Hazard Assessments for Sandy Coasts: Appraisal of Five Methodologies. *Journal of Coastal Research*, *35*(3), 574. Recovered from https://doi.org/10.2112/jcoastres-d-18-00083.1

Narra, P., Coelho, C., Sancho, F., & Palalane, J. (2017). CERA: An open-source tool for coastal erosion risk assessment. *Ocean and Coastal Management*, 142, 1-14. Recovered from https://doi.org/10.1016/j.ocecoaman.2017.03.013

Natesan, U., Parthasarathy, A., Vishnunath, R., Kumar, G. E. J., & Ferrer, V. A. (2015). Monitoring longterm shoreline changes along Tamil Nadu, India using geospatial techniques. *Aquatic Procedia*, *4*(Icwrcoe), 325-332. Recovered from https://doi.org/10.1016/j.aqpro.2015.02.044

Pollard, J. A., Spencer, T., & Brooks, S. M. (2019). The interactive relationship between coastal erosion and flood risk. *Progress in Physical Geography*, 43(4), 574-585. Recovered from https://doi.org/10.1177/0309133318794498

Smith, G. L., & Zartllo, G. A. (1990). Calculating long-term shoreline recession rates using aerial photographic and beach profiling techniques. *Journal of Coastal Research*, *6*(1), 111–120. Recovered from https://journals.flvc.org/jcr/article/view/78000

Stevens, A. J., Clarke, D., Nicholls, R. J., & Wadey, M. P. (2015). Estimating the long-term historic evolution of exposure to flooding of coastal populations. *Natural Hazards and Earth System Sciences*, 15(6), 1215-1229. Recovered from https://doi.org/10.5194/nhess-15-1215-2015

Thieler, E. R., & Hammar-Klose, E. S. (1999). National assessment of coastal vulnerability to sea-level rise. *Open-File Report 00-179*, 1.

Thieler, R., Himmelstoss, E., Zichichi, J., & Ayhan, E. (2009). *The Digital Shoreline Analysis System (DSAS) Version 4.0 - An ArcGIS extension for calculating shoreline change*. Recovered from https://doi.org/https://doi.org/10.3133/ofr20081278

Uysal, M., Polat, N., & Aydın, M. (2018). *Monitoring of coastal erosion of Karasu Coast in Black Sea*. In: Kallel, A., Ksibi, M., & Ben-Dhia, H. (ed.). Recovered from https://doi.org/10.1007/978-3-319-70548-4_470

Viavattene, C., Jiménez, J. A., Ferreira, O., Priest, S., Owen, D., & McCall, R. (2018). Selecting coastal hotspots to storm impacts at the regional scale: A coastal risk assessment framework. *Coastal Engineering*, 134(January, 2017), 33-47. Recovered from https://doi.org/10.1016/j.coastaleng.2017.09.002